

# Experimental and Thermodynamic Study of the Equilibria Between Ferrite, Austenite and Intermediate Phases in the Fe-Mo, Fe-W, and Fe-Mo-W Systems

GERNOT KIRCHNER, HANS HARVIG, AND BJÖRN UHRENIUS

The phase equilibria between ferrite and austenite and between ferrite and the intermediate  $R$ - and  $\mu$ -phases have been studied by subjecting high purity alloys of Fe-Mo, Fe-W, and Fe-Mo-W to well controlled heat treatments. The equilibrium compositions at the two-phase interfaces were measured with an electron microprobe. Some of the experimental results show reasonable agreement with previously reported values, but are believed to be of higher accuracy. The new experimental data were, together with available relevant thermodynamic information, evaluated in terms of mathematical models for the individual phases and the parameters thus obtained were then used to calculate the two-phase boundaries in the binary Fe-Mo, Fe-W, and ternary Fe-Mo-W systems. In the course of this study the free energy of formation of the  $R$  and  $\mu$  phases was also evaluated.

THE Fe-Mo and Fe-W phase diagrams have recently been examined in several investigations.<sup>1-4</sup> Hillert *et al.*<sup>1</sup> revised the  $\gamma$  loops and demonstrated that their shapes could be rather well described in terms of a dilute solution model. Their results were essentially confirmed by Sinha *et al.*<sup>2,3</sup> and Fisher *et al.*<sup>4</sup> Sinha *et al.*<sup>2</sup> found a new phase in the Fe-Mo system, which they called  $R$  and which was also identified by Rawlings and Newey.<sup>5</sup> Sinha *et al.*<sup>2,3</sup> also claim that a  $\lambda$  phase containing 66.7 at. pct Fe becomes stable in both the Fe-Mo and Fe-W systems at low temperatures. Even though this phase was not detected by Rawlings and Newey<sup>5</sup> in their investigation of the Fe-Mo system, both binary phase diagrams presented by Sinha *et al.*<sup>2,3</sup> seem to be essentially correct. They are therefore reproduced in Figs. 1 and 2 and show remarkable similarities although the  $R$  phase does not seem to exist in the Fe-W system.

The present investigation was started by Kirchner and Hammar<sup>6</sup> who attempted to carry out a more accurate determination of the  $\gamma$  loops by using carefully selected raw materials for their alloys, accurate temperature control during the equilibration heat treatment and careful analysis of the composition of the individual phases at two-phase interfaces by electron microprobe measurements. The investigation was then extended to include ternary alloys as well as the intermediate phases  $\mu$  and  $R$ . These experimental results are now reported and they will be analyzed together with all other relevant information available in terms of thermodynamic parameters, which in turn will be used to calculate the phase boundaries in the two binary systems Fe-Mo and Fe-W, and to some degree even in the ternary system Fe-Mo-W. It is suggested that phase boundaries evaluated in that way represent a much

more accurate compilation of the available information than the previously published phase diagrams, drawn by hand or computed by means of a Henry's law model, which is valid only for very dilute solutions.

## 1) EQUILIBRIA BETWEEN FERRITE AND AUSTENITE

### 1.1) Experimental

#### 1.1.1 MATERIALS, ALLOY PREPARATION, AND HEAT TREATMENTS

Five Fe-Mo and five Fe-W alloys were prepared using very pure metals, Table I. The alloys were induction melted in an atmosphere of purified argon and then poured into thick-walled copper molds. The resulting 12 by 12 mm rods were cleaned by grinding, chemically analyzed, Table II, then cut into pieces 5 by 5 by 10 mm and finally polished. The specimens were first cleaned in trichlorethylene *p.a.*, then immersed in an ultrasonic cleaner (alcohol as cleaning fluid) after which they were rinsed in 99.5 vol pct alcohol, dried and put into alumina crucibles, covered with a smaller crucible, which served as a lid and vacuum sealed (approx.  $10^{-4}$  atm) in carefully cleaned transparent quartz tubes. The capsules were equilibrated during an appropriate time, Tables III and IV, in heat treating units designed to give a very constant temperature. The stability was  $\pm 0.4$  K or better. The temperature was measured by calibrated thermocouples and a Leeds and Northrup 8686-2 mV potentiometer combined with a high quality ice point reference chamber. After the heat treatment the alloys were quenched by breaking the capsules in brine. The specimens were cut in half and the new surface was prepared and examined metallographically. Alloys, whose compositions were within the two-phase region, were selected for the microprobe measurements.

#### 1.1.2) DIFFUSION COUPLE EXPERIMENTS IN THE FE-W SYSTEM

Two alloys with 0.607 and 1.55 at. pct W, respectively, were rolled to strips 0.25 mm thick and spot-welded

GERNOT KIRCHNER and BJÖRN UHRENIUS are Assistant Professors at the Division of Physical Metallurgy, Royal Institute of Technology, Stockholm, Sweden. HANS HARVIG, formerly Assistant Professor, the Division of Physical Metallurgy, Royal Institute of Technology, Stockholm, Sweden, is now with the Steel Development of Gränges Steel, Oxelösund, Sweden.

Manuscript submitted July 14, 1972.

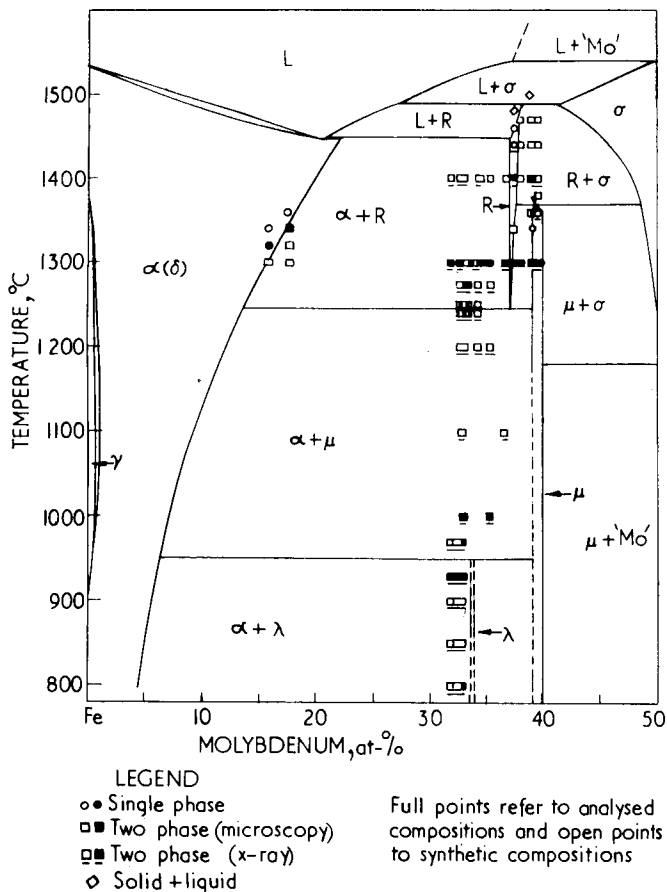


Fig. 1—The Fe-Mo phase diagram according to Sinha, Buckley, and Hume-Rothery.<sup>2</sup>

together at two points approximately 10 mm apart. These specimens were vacuum sealed in quartz capsules and equilibrated at 1273 K during 1098 h. Contact was then usually established over the whole area between the welds. After quenching in brine and cutting in half, the concentration profiles were determined by electron microprobe analysis perpendicular to the plane of contact. We do not want to emphasize the use of diffusion couples for phase diagram studies but believe that this technique can be an interesting complement to the usual method employing alloys whose composition is within the two-phase region already at the beginning of the heat treatment.

### 1.1.3) ELECTRON MICROPROBE ANALYSIS AND RESULTS

The concentration of the alloying elements in ferrite and austenite was determined by electron microprobe analysis using a CAMECA microprobe type M 46. The spectrometers were adjusted by means of the pure metals, Table I. The microprobe was calibrated using the alloys, Table II, which were all ferritic at room temperature, as reference materials. The measurements were carried out at a series of points along a line perpendicular to the  $\alpha/\gamma$  phase boundary. The resulting concentration profiles were in all cases sufficiently long and flat to allow safe extrapolation to the interface. An example is presented in Fig. 3. At least four calibrations were performed during the determination of one concentration profile. The results

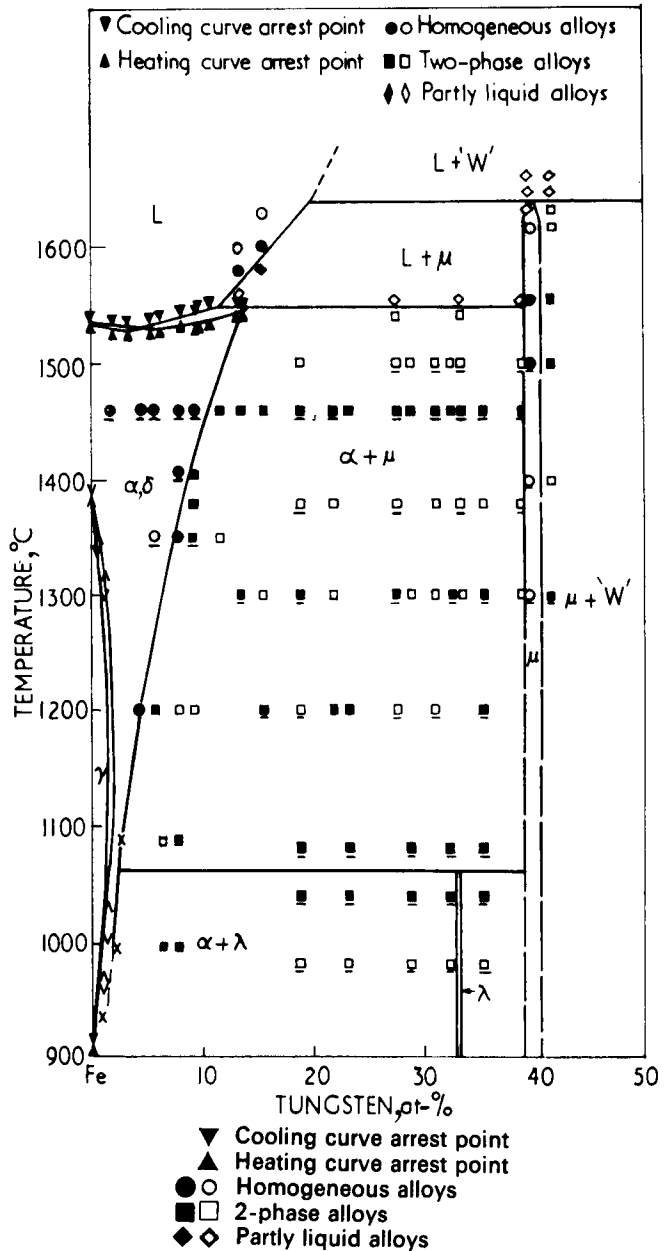


Fig. 2—The Fe-W phase diagram according to Sinha and Hume-Rothery.<sup>3</sup>

shown in Tables III and IV are the average of at least ten concentration profiles.

### 1.2) Discussion of the Experimental $\gamma$ Loop Studies

Hillert *et al.*<sup>1</sup> published preliminary measurements of the  $\gamma$  loop in the Fe-Mo and Fe-W systems based upon equilibrated two-phase alloys. Sinha *et al.*<sup>2,3</sup> and Fisher *et al.*<sup>4</sup> have recently made attempts to determine the same equilibria using dynamic methods. However, Sinha *et al.*<sup>2,3</sup> did not measure the width of the loops at the vertex and their experiments can not even be interpreted as a determination of the allotropic line at the vertex. Fisher *et al.*<sup>4</sup> have studied the width of the  $\gamma$  loops close to the vertex by a dynamic method. Detailed information about their experimental procedures and methods of evaluation is lacking. For example it was not reported which velocities were employed and if they were varied at all. Furthermore it seems

**Table I. Analyses of Metals Used for  $\gamma$  Loop Studies**

Impurities	Concentration, ppm, of Impurities		
	Electrolytic Iron	Molybdenum 99.96 Wt Pct Mo	Tungsten >99.97 Wt Pct W
Al	<10	<10	15
C	20	10	30
Ca	n.d.	<10	<10
Co	50	<10	<10
Cr	<10	<10	10
Cu	10	<10	10
Fe	—	<40	15
H	n.d.	3	<5
Mg	n.d.	<10	<10
Mn	<10	<10	<10
Mo	<10	—	<60
N	20	3	20
Ni	40	<10	10
O	340	200	17
P	<10	n.d.	n.d.
S	70	n.d.	n.d.
Si	10	<10	<10
Sn	n.d.	<20	<10
Ti	<10	n.d.	n.d.
V	<10	n.d.	n.d.
Zr	n.d.	n.d.	<10

n.d.: Not determined.

**Table II. Composition of Alloys Used for  $\gamma$  Loop Studies**

a) Fe-Mo Alloys		
No.	At. Pct Mo	Wt Pct C
K23	1.02	0.002
K24	1.42	0.002
K25	1.78	0.003
K56	1.95	0.0017
K50	2.19	0.0015
b) Fe-W Alloys		
No.	At. Pct W	Wt Pct C
K31	1.03	0.0018
K32	1.32	0.0018
K33	1.54	0.0016
K57	1.83	0.0015
K49	1.97	0.0015

**Table III. The Distribution of Molybdenum Between Ferrite and Austenite Determined by Electron Microprobe Analysis of Two-Phase Alloys**

Heat Treatment		Mole Fraction of Molybdenum in	
Temperature,* K	Time, hrs	Austenite	Ferrite
1263	936	0.0110 ± 0.0002	0.0148 ± 0.0003
1310	1248	0.0134 ± 0.0003	0.0185 ± 0.0004
1410	768	0.0169 ± 0.0003	0.0226 ± 0.0003
1530	15	0.0127 ± 0.0004	0.0169 ± 0.0005
1573	9	0.0102 ± 0.0002	0.0131 ± 0.0003

\*All temperatures given in this study are according to the IPTS-1948.

to the present authors that the method of evaluation used by Fisher *et al.*<sup>4</sup> in the temperature range of the vertex is rather uncertain and depending on assumptions which might not be justified. Only Hillert *et al.*<sup>1</sup> have hitherto studied the width at the vertex by a static method, but their work was of preliminary nature. In view of the shortcomings of the experimental techniques

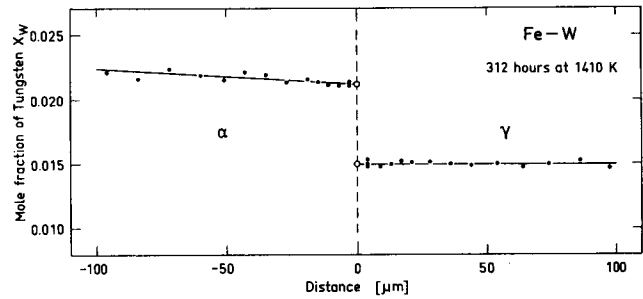


Fig. 3—Typical concentration profile, determined by electron microprobe analysis of a Fe-W specimen equilibrated for 312 h at 1410 K.

**Table IV. The Distribution of Tungsten Between Ferrite and Austenite Determined by Electron Microprobe Analysis of Two-Phase Alloys**

Heat Treatment		Mole Fraction of Tungsten in	
Temperature,* K	Time, hrs	Austenite	Ferrite
1263	936	0.0100 ± 0.0002	0.0143 ± 0.0003
1310	1248	0.0122 ± 0.0002	0.0172 ± 0.0003
1410	312	0.0152 ± 0.0003	0.0211 ± 0.0003
1551	10	0.0109 ± 0.0002	0.0142 ± 0.0005

\*All temperatures given in this study are according to the IPTS-1948.

used by the previous authors it is surprising that their results agree so well with each other. According to our opinion this agreement should be regarded as fortuitous and the present results, based upon very pure starting materials, carefully controlled equilibration heat treatments, and precise electron microprobe calibration, should be preferred and will be used for the thermodynamic calculation carried out in the next section. The present results are around 0.3 at. pct higher than the previous ones.

### 1.3) Thermodynamic Calculations

#### 1.3.1) THERMODYNAMIC MODELS FOR FERRITE AND AUSTENITE

In their investigation of binary iron-base alloys Hillert *et al.*<sup>1</sup> applied a regular solution model. However, in the case of Fe-Mo and Fe-W information was scarce and they decided therefore to apply the dilute-solution approximation which conforms to Henry's law. The same model was used by Sinha *et al.*<sup>2,3</sup> and Fisher *et al.*<sup>4</sup> although more information was available by that time. An attempt to use a better approximation and to evaluate the thermodynamic parameters describing the solutions was recently undertaken in the Fe-Zn,<sup>7</sup> Fe-Cu,<sup>8</sup> and Fe-Cr<sup>9</sup> systems and the same approach will be made in the present investigation.

The regular solution approximation yields the following expression for the integral molar free energy of ferrite or austenite in the Fe-Mo-W system:

$$G_m = X_{Fe} {}^0G_{Fe} + X_{Mo} {}^0G_{Mo} + X_W {}^0G_W + RT(X_{Fe} \ln X_{Fe} + X_{Mo} \ln X_{Mo} + X_W \ln X_W) + {}^E G_m \quad [1]$$

where

$${}^E G_m = X_{Fe} X_{Mo} A_{FeMo} + X_{Fe} X_W A_{FeW} + X_{Mo} X_W A_{MoW} \quad [2]$$

The partial molar free energies are then obtained as follows:

$$\bar{G}_i = {}^0G_i + RT \ln X_i + {}^E G_i \quad [3]$$

where  $i$  stands for Fe, Mo, and W, respectively. In view of Eq. [2], the following expressions are obtained for the partial molar excess free energies  ${}^E G_i$ :

$${}^E G_{Fe} = X_{Mo}(1 - X_{Fe})A_{FeMo} + X_W(1 - X_{Fe})A_{FeW} - X_{Mo}X_W A_{MoW} \quad [4]$$

$${}^E G_{Mo} = X_{Fe}(1 - X_{Mo})A_{FeMo} - X_{Fe}X_W A_{FeW} + X_W(1 - X_{Mo})A_{MoW} \quad [5]$$

$${}^E G_W = -X_{Fe}X_{Mo}A_{FeMo} + X_{Fe}(1 - X_W)A_{FeW} + X_{Mo}(1 - X_W)A_{MoW} \quad [6]$$

The conditions for equilibrium are:

$$\bar{G}_i^{bcc} = \bar{G}_i^{fcc} \quad [7]$$

### 1.3.2) EVALUATION OF THE THERMODYNAMIC PARAMETERS FOR FERRITE AND AUSTENITE

Some of the quantities needed for the calculation can be obtained from the literature. The free energy difference  ${}^0G_{Fe}^{fcc} - {}^0G_{Fe}^{bcc}$  between the bcc and fcc state of pure iron has been tabulated by many authors and the values published by Orr and Chipman<sup>10</sup> will be used here. Kaufman<sup>11</sup> has estimated the corresponding quantities for molybdenum and tungsten and found:

$${}^0G_{Mo}^{fcc} - {}^0G_{Mo}^{bcc} = {}^0G_W^{fcc} - {}^0G_W^{bcc} = 2500 + 0.15T \text{ [cal mole}^{-1}] \quad [8]$$

$A_{FeMo}^{bcc}$  in ferrite was evaluated by Nishizawa<sup>12</sup> and a mean value of  $A_{FeMo}^{bcc} = 4250 \text{ cal mole}^{-1}$  is obtained from his work.\*

\*The energy unit used throughout the present study is the thermochemical calorie. 1 cal thermochemical = 4.1840 J.

$A_{FeW}^{bcc}$  in ferrite can be calculated by considering the equilibrium between a liquid Fe-W phase (denoted by  $L$ ) and almost pure solid tungsten at 1913 K. The equilibrium compositions are  $X_W^L = 0.163$  according to Schneider and Vogel<sup>13</sup> and  $X_W^{bcc} = 0.974$  reported by Sykes.<sup>14</sup> Kaufman<sup>15</sup> has suggested:

$${}^0G_W^L - {}^0G_W^{bcc} = 7300 - 2.0T \text{ [cal mole}^{-1}] \quad [9]$$

The condition  $\bar{G}_W^L = \bar{G}_W^{bcc}$  will thus give a value of  $A_{FeW}^L = 4720 \text{ cal mole}^{-1}$ . Assuming this parameter to be independent of temperature, the minimum on the liquidus at  $X_W = 0.044$  and 1802 K according to Sinha and Hume-Rothery<sup>3</sup> can be utilized by means of the equal free energy condition,  $G_m^L = G_m^{bcc}$ , which yields:

$$X_{Fe} {}^0G_{Fe}^L + X_W {}^0G_W^L + X_{Fe}X_W A_{FeW}^L = X_{Fe} {}^0G_{Fe}^{bcc} + X_W {}^0G_W^{bcc} + X_{Fe}X_W A_{FeW}^{bcc} \quad [10]$$

By inserting the parameter values already derived and by employing the following expression:

$${}^0G_{Fe}^L - {}^0G_{Fe}^{bcc} = 1.824(1809 - T) \text{ [cal mole}^{-1}] \quad [11]$$

which is in agreement with the enthalpy of melting  $\Delta H_{Fe}^{bcc \rightarrow L} = 3300 \text{ cal mole}^{-1}$  reported by Ferrier and Olette,<sup>16</sup> a value of  $A_{FeW}^{bcc} = 9040 \text{ cal mole}^{-1}$  is obtained. A similar evaluation can be carried out at the peri-

itectic horizontal at 1821 K where  $X_W^{bcc} = 0.143$  and  $X_W^L = 0.112$  according to Sinha and Hume-Rothery.<sup>3</sup> Since this two-phase field is rather narrow, the equal free energy condition can be assumed to hold at  $X_W = (X_W^L + X_W^{bcc})/2$  and will now yield  $A_{FeW}^{bcc} = 8740 \text{ cal mole}^{-1}$  in close agreement with the previous calculations. A value of  $A_{FeW}^{bcc} = 9000 \text{ cal mole}^{-1}$  may thus seem reasonable and is assumed to hold independent of temperature.

The parameters for the  $\gamma$  phase can now be evaluated from the experimental information on the  $\alpha/\gamma$  equilibria reported in a previous section. In order to minimize the effect of experimental errors, it is then advantageous not to use Eq. [7] but to apply the equal free energy condition  $G_m^{fcc} - G_m^{bcc} = 0$  somewhere in the middle of the  $(\alpha + \gamma)$  two-phase field and thus to obtain an equation analogous to Eq. [10]. As the  $(\alpha + \gamma)$  two-phase field is narrow, the equal free energy condition can be applied at  $X_M = (X_M^{bcc} + X_M^{fcc})/2$ , where  $M$  denotes molybdenum or tungsten. The differences  $A_{FeM}^{fcc} - A_{FeM}^{bcc}$  were evaluated in this way for all temperatures listed in the Tables III and IV and can be represented by:

$$A_{FeMo}^{fcc} - A_{FeMo}^{bcc} = -1935 \text{ [cal mole}^{-1}], \quad [12]$$

independent of temperature and

$$A_{FeW}^{fcc} - A_{FeW}^{bcc} = -1210 - 0.45T \text{ [cal mole}^{-1}] \quad [13]$$

By combination with the parameters evaluated previously,  $A_{FeMo}^{fcc} = 2315 \text{ cal mole}^{-1}$  and  $A_{FeW}^{fcc} = 7800 - 0.45T \text{ [cal mole}^{-1}]$  are thus obtained.

In the classical regular solution model, it is assumed that the  $A$  parameter is independent of temperature. In the above evaluation of various parameters this assumption was accepted except for the case of  $A_{FeW}^{fcc} - A_{FeW}^{bcc}$ , where the experimental data combined with the phase stability accepted for pure tungsten, Eq. [8], strongly indicate a temperature dependency. In the strict sense, the term "regular solution" should not be used unless the  $A$  parameter is independent of temperature. However, all the equations relating to phase equilibria which were presented in section 1.3.1 refer to isothermal conditions and are valid independent of how the  $A$  parameters vary with temperature. As a consequence it will cause no complications if it would become necessary to relax the restriction of constant  $A$  parameters in view of new experimental information indicating temperature dependency. The term "regular solution" is sometimes extended to include such a model as well, which for instance was applied to phase equilibria by Porter<sup>17</sup> and in the German scientific literature is often called "PORTERScher Ansatz" (Porter's formulation).

### 1.3.3) CALCULATION OF THE $\alpha/\gamma$ PHASE BOUNDARIES

All thermodynamic quantities needed in order to calculate the  $\gamma$  loops in the binary Fe-Mo and Fe-W systems are now known. The computation was carried out using a programmable electronic desk calculator in a way described by Kirchner *et al.*<sup>7</sup> The results are shown in Figs. 4 and 5. It is interesting to note, that there is good agreement between the experimental data and the calculated  $\gamma$  loops, in spite of the fact that the experimentally determined width of the  $\gamma$  loops was not

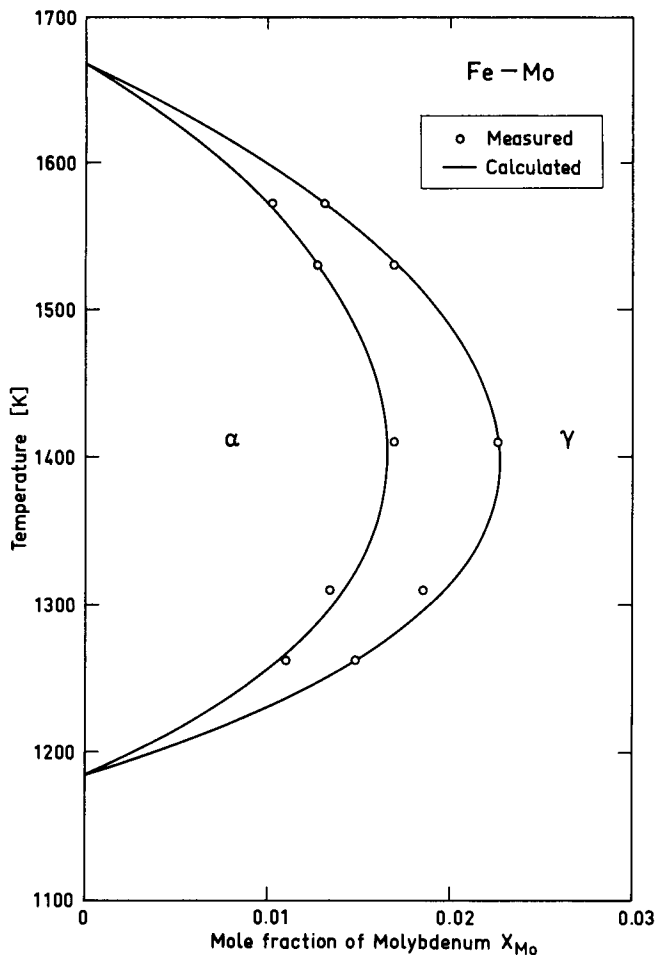


Fig. 4—The  $\gamma$  loop in the Fe-Mo system.

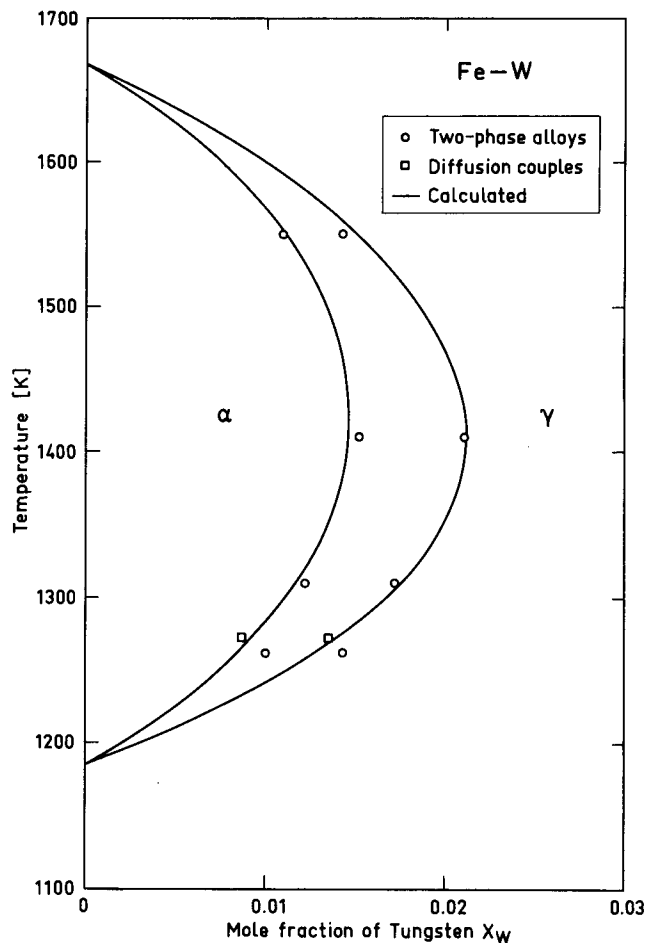


Fig. 5—The  $\gamma$  loop in the Fe-W system.

used in the evaluation of the parameters. This justifies the choice of the thermodynamic model and demonstrates the usefulness of the equal free energy condition.

Two parameters,  $A_{MoW}^{bcc}$  and  $A_{MoW}^{fcc}$ , remain to be determined in order to allow the calculation of the  $\alpha/\gamma$  phase boundaries in the ternary Fe-Mo-W system. However, these parameters will only have a slight influence when both the molybdenum and tungsten contents are low and the calculations can thus be carried out neglecting the terms containing  $A_{MoW}^{bcc}$  and  $A_{MoW}^{fcc}$ . The results obtained for 1373 K are presented in Fig. 6.

## 2) EQUILIBRIA BETWEEN FERRITE AND INTERMEDIATE PHASES

### 2.1) Experimental

The alloys, Table V, used in the study of the equilibria between ferrite and intermediate phases were produced and treated in a way described earlier in this paper. The accuracy of temperature measurement and control, however, was not so good here. It was estimated to  $\pm 3$  K.

The concentrations of the alloying elements were also in this case measured by means of the CAMECA microprobe mentioned above. For low contents the same calibration technique was used as for the  $\gamma$  loop studies but some theoretical calibration procedure is required at higher concentrations of the alloying ele-

Table V. Composition of Alloys Used in Studying the Equilibria Between Ferrite and Intermediate Phases

No.	Contents, Wt Pct		Contents, At. Pct	
	Mo	W	Mo	W
H1*	40	—	28	—
H25*	30	10	22	3.8
H23*	20	20	15	7.8
H24*	10	30	7.8	12
H22*	—	40	—	17
H17	19.75	—	12.53	—
H20	14.90	5.10	9.61	1.77
H19	10.16	9.98	6.66	3.41
H21	4.94	15.10	3.29	5.25
H18	—	19.50	—	6.84
H12	9.97	—	6.56	—
H15	7.50	2.53	4.59	0.81
H14	5.00	5.03	3.08	1.62
H16	2.50	7.64	1.55	2.48
H13	—	9.94	—	3.24

\*Alloys H1, H25, H23, H24, and H22 were not analyzed chemically.

ments since it is very difficult to produce single-phase specimens of higher alloying contents than approximately 20 wt pct. The following calibration formula according to Ziebold and Ogilvie<sup>18</sup> was used:

$$C_M = \frac{100 I \beta}{I(\beta - 1) + 1} \text{ [wt pct]} \quad [14]$$

where  $C_M$  is the concentration of molybdenum or

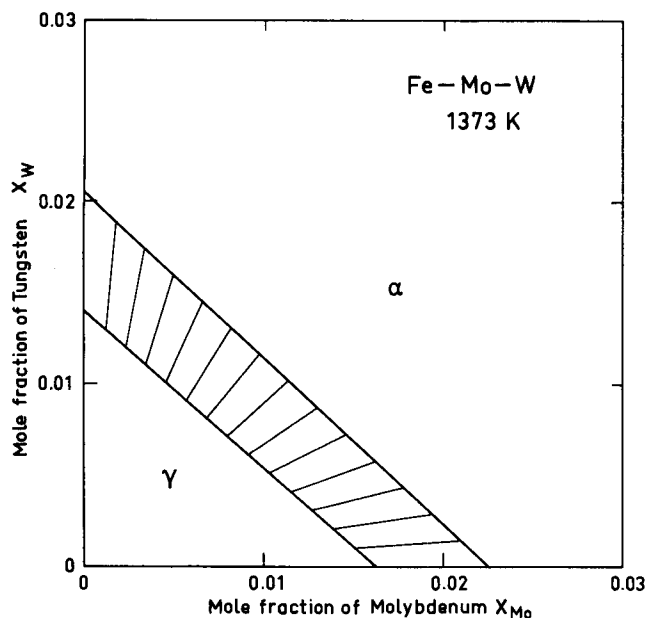


Fig. 6—The  $\alpha/\gamma$  equilibrium in the Fe-Mo-W system at 1373 K.

Table VI. The Distribution of Molybdenum and Tungsten Between Ferrite and Intermediate Phases Determined by Electron Microprobe Analysis

Alloy No.	Heat Treatment		Phases	Mole Fraction of Mo and W in			
	Temperature, K	Time, hrs		Ferrite		Intermediate Phases	
H1	1373	720	$\alpha + \mu$	0.0912	—	0.400	—
H25	1373	720	$\alpha + \mu$	0.0788	0.0078	0.321	0.071
H23	1373	720	$\alpha + \mu$	0.0664	0.0213	0.221	0.164
H24	1373	720	$\alpha + \mu$	0.0302	0.0252	0.127	0.258
H22	1373	720	$\alpha + \mu$	—	0.0370	—	0.390
H1	1578	120	$\alpha + R$	0.171	—	0.361	—
H25	1578	120	$\alpha + R$	0.121	0.0205	0.283	0.082
H23	1578	120	$\alpha + \mu$	0.0877	0.0281	0.211	0.180
H24	1578	120	$\alpha + \mu$	0.0480	0.0501	0.109	0.286
H22	1578	120	$\alpha + \mu$	—	0.0641	—	0.401

\*All temperatures given in this study are according to the IPTS-1948.

tungsten in percent by weight,  $I$  is the relative intensity,\* and  $\beta = 1.45 \pm 0.05$  for both molybdenum and

$$I = \frac{\text{Intensity from specimen} - \text{Intensity from background}}{\text{Intensity from standard} - \text{Intensity from background}}$$

tungsten. This value of  $\beta$  was derived from single-phase alloys containing up to 20 wt pct Mo or W, respectively.

When analyzing phases containing both molybdenum and tungsten a complication arises caused by the effect of tungsten on molybdenum. This was corrected for by multiplying the measured  $C_M$ -value with a factor  $B$ , which was assumed to depend upon the proportion of  $C_W/C_{Mo}$ . Values of  $B$  were determined experimentally at low alloy contents employing single-phase alloys with different values of  $C_W/C_{Mo}$  and then used at those higher contents which yield the same proportions. No effect of molybdenum on tungsten was observed.

The intermediate phases were isolated electrolytically and then identified by taking Guinier photograms. The  $R$  phase was detected in alloys H1 and H25 after

heat treatment at 1578 K. In all other alloys the intermediate phase observed was  $\mu$ .

## 2.2) Results

The experimental results are presented in Table VI. The data obtained for the binary systems are in agreement with the results of Sinha *et al.*<sup>2,3</sup> In particular, they found that the  $\mu$  phase has iron contents between 60.0 and 61.0 at. pct in the Fe-Mo and 59.5 and 60.9 at. pct in the Fe-W system. All the results in Table VI, including those for ternary alloys give iron contents between 59.9 and 61.5 at. pct. The difference between these values is thus very small and within the uncertainty of the present measurements. As a consequence it seems reasonable to treat the  $\mu$  phase as a stoichiometric phase with 60 at. pct Fe and the thermodynamic calculations in the next section are based on such an assumption. The ternary data in Table VI will then be adjusted to conform to this assumption by multiplying the molybdenum and tungsten contents with a common factor evaluated for each measurement. These factors were only slightly larger than unity.

Sinha *et al.*<sup>2</sup> found that the  $R$  phase in the Fe-Mo system has an iron content between 62.6 and 63.4 at. pct Fe at 1573 K. Table VI gives a value of 63.9 at. pct Fe for an Fe-Mo and 63.5 at. pct Fe for an Fe-Mo-W alloy. It may thus seem reasonable to adopt a value of 63 at. pct Fe for this phase. According to Sinha and Hume-Rothery<sup>3</sup> the  $R$  phase does not seem to exist in the Fe-W system, which was confirmed during the course of this study.

The solubilities of the  $\mu$  and  $R$  phases in ferrite, presented in Table VI, are in good agreement with the data according to Sinha *et al.*<sup>2,3</sup> and both sources of information will be used in the thermodynamic treatment of these equilibria.

## 2.3) Thermodynamic Model for the Intermediate Phases

As already explained, it will be assumed that the intermediate phases have constant iron contents. It is then reasonable to treat them as stoichiometric phases of the type  $Fe_a(Mo,W)_b$  and to define the molar free energies  ${}^0G_{Fe_a/b Mo}^{ip}$  and  ${}^0G_{Fe_a/b W}^{ip}$  in each binary system. The composition of a ternary phase will be described by the concentration parameters:

$$Y_{Mo} = X_{Mo}/(X_{Mo} + X_W) = X_{Mo}(a+b)/b \quad [15a]$$

$$Y_W = X_W/(X_{Mo} + X_W) = X_W(a+b)/b \quad [15b]$$

and its integral molar free energy is then defined by the following expression:

$$G_m = Y_{Mo} {}^0G_{Fe_a/b Mo} + Y_W {}^0G_{Fe_a/b W} + RT [Y_{Mo} \ln Y_{Mo} + Y_W \ln Y_W] + Y_{Mo} Y_W A_{MoW}^{ip} \quad [16]$$

where the parameter  $A_{MoW}^{ip}$  represents the interaction between molybdenum and tungsten in the intermediate phase under consideration. The equilibrium between ferrite and the intermediate phase is described by the following two equations:<sup>19</sup>

$$\begin{aligned}
{}^0G_{Fe_{a/b}Mo}^{ip} &= {}^0G_{Mo}^{bcc} - \frac{a}{b} {}^0G_{Fe}^{bcc} + Y_{Mo}^2 A_{MoW}^{ip} \\
&= RT \ln X_{Mo}/Y_{Mo} + \frac{a}{b} RT \ln X_{Fe} \\
&\quad + E_{G_{Mo}}^{bcc} + \frac{a}{b} E_{G_{Fe}}^{bcc} \quad [17]
\end{aligned}$$

$$\begin{aligned}
{}^0G_{Fe_{a/b}W}^{ip} &= {}^0G_W^{bcc} - \frac{a}{b} {}^0G_{Fe}^{bcc} + Y_{Mo}^2 A_{MoW}^{ip} \\
&= RT \ln X_W/Y_W + \frac{a}{b} RT \ln X_{Fe} \\
&\quad + E_{G_W}^{bcc} + \frac{a}{b} E_{G_{Fe}}^{bcc} \quad [18]
\end{aligned}$$

All the  $X$  refer to ferrite and all the  $Y$  to the intermediate phase. The values of the partial molar excess free energies for ferrite can be obtained from Eqs. [4] to [6].

#### 2.4) Equilibria Between Ferrite and the $R$ and $\mu$ Phases in the Fe-Mo System

For the binary Fe-Mo system Eq. [17] simplifies considerably:

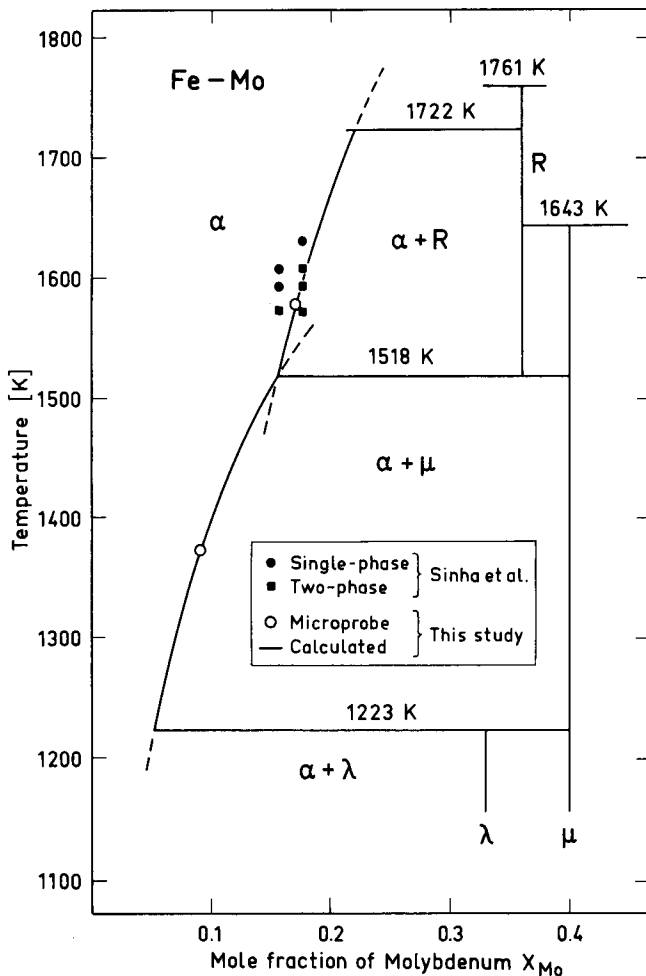


Fig. 7—The  $\alpha/R$  and  $\alpha/\mu$  equilibria in the Fe-Mo system. The  $\gamma$  loop, shown in Fig. 4, is not given here.

$$\begin{aligned}
{}^0G_{Fe_{a/b}Mo}^{ip} &= \frac{a}{b} {}^0G_{Fe}^{bcc} - {}^0G_{Mo}^{bcc} = \frac{a}{b} RT \ln X_{Fe} \\
&\quad + RT \ln X_{Mo} + (X_{Fe}^2 + \frac{a}{b} X_{Mo}^2) A_{FeMo}^{bcc} \quad [19]
\end{aligned}$$

The parameter  $A_{FeMo}^{bcc}$  is already known and the right-hand side of Eq. [19] can thus be evaluated from the solubility of the intermediate phases in ferrite. For the  $R$  phase, this computation was carried out at 1578 K using the solubility of  $X_{Mo} = 0.171$  presented in Table VI and at the peritectic temperature using  $X_{Mo} = 0.22$  according to Gibson *et al.*<sup>20</sup> Assuming a linear temperature dependency of the left-hand side of Eq. [19], the following expression was obtained:

$${}^0G_{Fe_{1.70}Mo}^R - 1.70 {}^0G_{Fe}^{bcc} - {}^0G_{Mo}^{bcc} = -265 - 1.99T \quad [cal \text{ mole}^{-1}] \quad [20]$$

Using this relation, the whole solubility curve for the  $R$  phase was calculated from Eq. [19] on a programmable electronic desk calculator in a way described earlier.<sup>7</sup> The result is plotted in Fig. 7.

A similar evaluation was carried out for the  $\mu$  phase using  $X_{Mo} = 0.0912$  at 1373 K from Table VI and  $X_{Mo} = 0.154$  at the eutectoid temperature of 1518 K obtained from the solubility curve of the  $R$  phase calculated in the preceding paragraph and plotted in Fig. 7. Assuming a linear temperature dependency the following expression was found:

$${}^0G_{Fe_{1.5}Mo}^\mu - 1.5 {}^0G_{Fe}^{bcc} - {}^0G_{Mo}^{bcc} = -4900 + 1.12T \quad [cal \text{ mole}^{-1}] \quad [21]$$

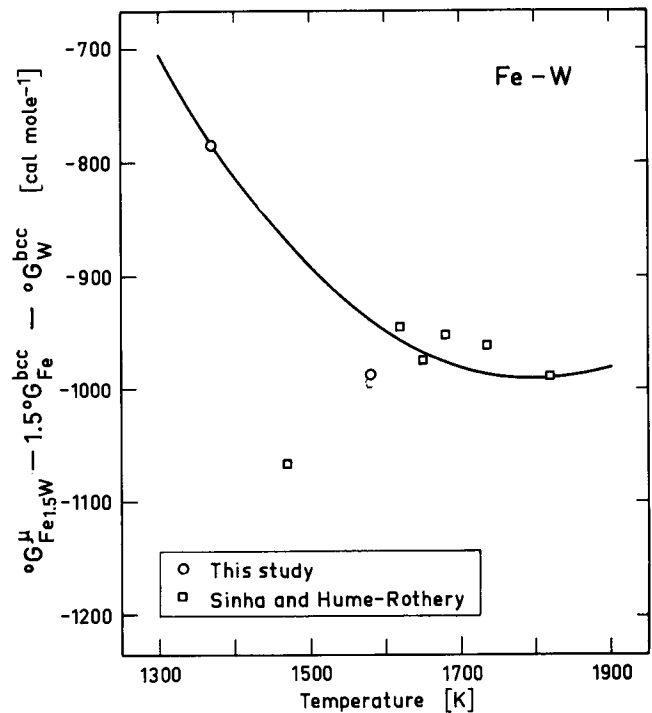


Fig. 8—The standard free energy of formation of the  $\mu$  phase ( $Fe_{1.5}W$ ) calculated from the data presented in this study, Table VI, and from the  $\alpha/\mu$  phase boundary chosen by Sinha and Hume-Rothery, Fig. 2. The curve is given by:

$${}^0G_{Fe_{1.5}W}^\mu - 1.5 {}^0G_{Fe}^{bcc} - {}^0G_W^{bcc} = 5636 - 31.25T + 3.678T \ln T \quad [cal \text{ mole}^{-1}]$$

Using this equation, the solubility of the  $\mu$  phase in ferrite can be calculated from Eq. [19]. This result is also plotted in Fig. 7.

### 2.5) Equilibrium Between Ferrite and the $\mu$ Phase in the Fe-W System

The same method as in the preceding section was applied. The parameter  $A_{FeW}^{bcc}$  is already known from the calculation of the  $\alpha/\gamma$  equilibrium. All the solubility determinations given in Table VI and in the paper by Sinha and Hume-Rothery<sup>3</sup> were used and the result of the evaluation is presented in Fig. 8. The data scatter considerably. A line was selected by paying most attention to the measurements which were regarded as the most reliable ones. It is described by the following equation:

$${}^{\circ}G_{Fe_{1.5}W}^{\mu} - 1.5 {}^{\circ}G_{Fe}^{bcc} - {}^{\circ}G_{W}^{bcc} = 5636 - 31.25T + 3.678T \ln T \quad [\text{cal mole}^{-1}] \quad [22]$$

Using this expression, the solubility of the  $\mu$  phase in ferrite was recalculated. The result is plotted in Fig. 9 and there compared with the experimental information.

### 2.6) Equilibria between Ferrite and the $R$ and $\mu$ Phases in the Fe-Mo-W System

The experimental information on the  $\alpha/\mu$  equilibrium concerns rather low molybdenum and tungsten contents in ferrite and, thus it does not seem justified to use

that information to estimate the interaction energy between molybdenum and tungsten in ferrite. Instead, the value  $A_{MoW}^{bcc} = 0 \text{ cal mole}^{-1}$  will be used which is in agreement with the results obtained by Chekhovskoi *et al.*<sup>21</sup> on a binary W-Mo alloy.

The  $A$  parameter for the  $\mu$  phase can now be evaluated from the experimental data in Table VI using either one of Eqs. [17] or [18]. However, considering the fact that some of the experimental error might be eliminated when the ratio  $X_{Mo}Y_W/X_WY_{Mo}$  is calculated, the evaluation was performed using a relation obtained by taking the difference between Eqs. [17] and [18]. An  $A_{MoW}^{\mu}$  value was computed from each experimental tie-line at 1373 K and results ranging from  $-3600$  to  $+1500 \text{ cal mole}^{-1}$  were obtained. The solution between the two binary  $\mu$ -phases is thus close to ideal. Instead of simply choosing the average of the values obtained, calculations of the whole two-phase field were performed using a series of  $A_{MoW}^{\mu}$  values within the experimental range. They all reproduced the slope of the tie-lines fairly well but gave distinctly different shapes of the solubility line for the  $\mu$  phase in ferrite. The value of  $A_{MoW}^{\mu} = 500 \text{ cal mole}^{-1}$  gave the best agreement with the experimental measurements of the  $\alpha/\mu$  equilibrium and was thus selected.

The experimental information on the  $\alpha/\mu$  equilibrium at 1578 K was more meagre and was suspected to be less accurate. However, in view of the result from 1373 K, it was expected that the  $A_{MoW}^{\mu}$ -parameter at 1578 K should also be close to zero. A series of low values were thus tested and  $A_{MoW}^{\mu} = -700 \text{ cal mole}^{-1}$  was finally chosen because it gave the best agreement for the solubility of the  $\mu$  phase in ferrite. No attention was paid to the slope of the experimentally determined ( $\alpha + \mu$ ) tie-lines at this temperature.

For the  $R$  phase, two parameters are unknown because it does not exist in the binary Fe-W system. Both of the Eqs. [17] and [18] are thus needed. From Eq. [17]  $A_{MoW}^R = -274 \text{ cal mole}^{-1}$  at 1578 K was ob-

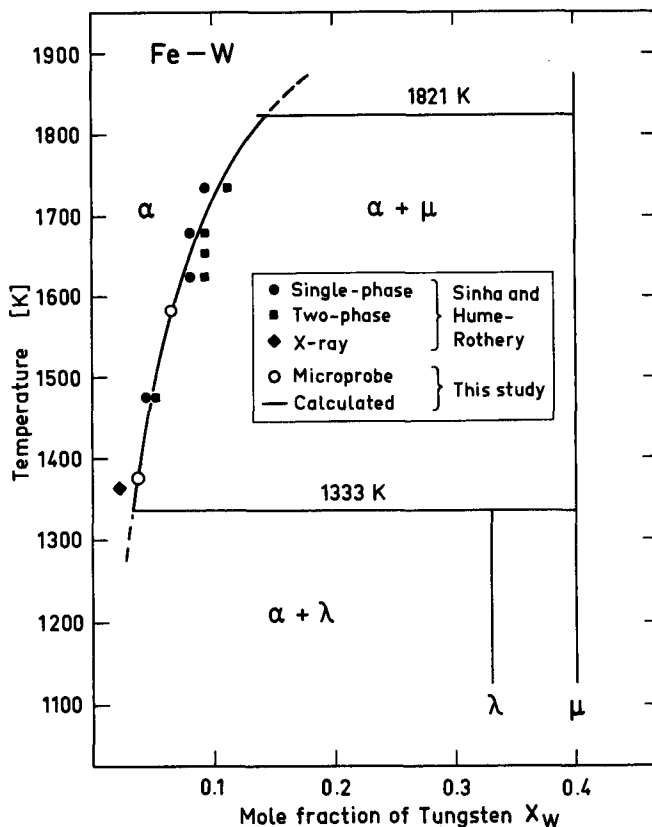


Fig. 9—The  $\alpha/\mu$  equilibrium in the Fe-W system. The  $\gamma$  loop shown in Fig. 5, is not given here.

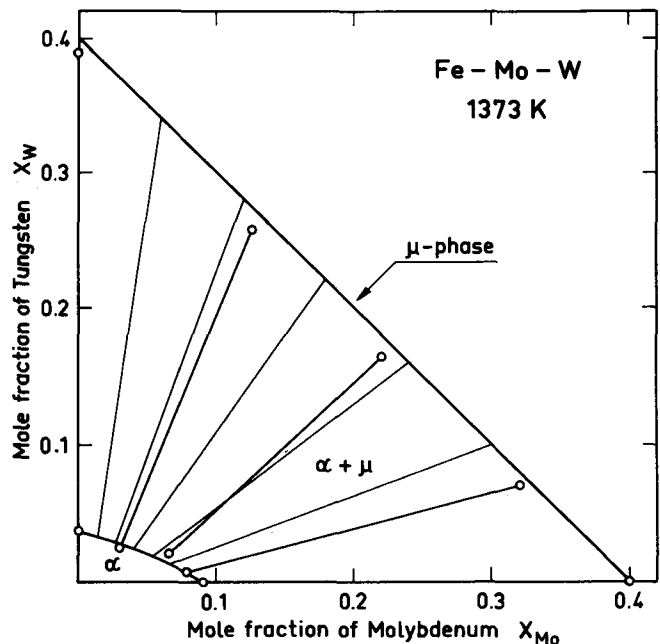


Fig. 10—The  $\alpha/\mu$  equilibrium in the Fe-Mo-W system at 1373 K.



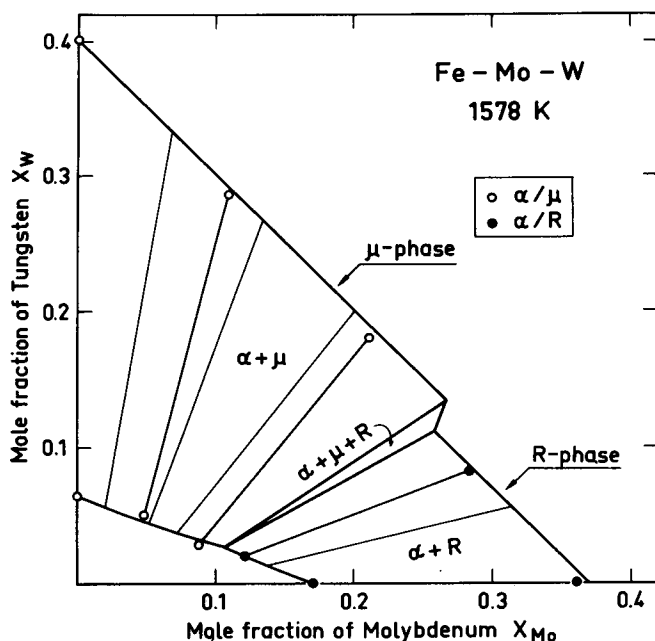


Fig. 11—The  $\alpha/\mu$  and  $\alpha/R$  equilibria in the Fe-Mo-W system at 1578 K.

tained and Eq. [18] gave  ${}^0G_{\text{Fe}_{1.70}\text{W}}^R - 1.7{}^0G_{\text{Fe}}^{\text{bcc}} - {}^0G_{\text{W}}^{\text{bcc}} = -867 \text{ cal mole}^{-1}$ .

All parameters necessary for the calculation of the ternary  $\alpha/\mu$  and  $\alpha/R$  equilibria are now available. The result of that calculation is compared with the experimental measurements in Figs. 10 and 11. The fairly good agreement indicates that the experimental data can be well represented by the parameter values derived in this way. It should be noted that the exact position of the  $(\alpha + \mu + R)$  three-phase triangle was not checked experimentally.

In view of the higher complexity, the calculations of the ternary Fe-Mo-W system were carried out on an electronic computer.

### 3) SUMMARY AND CONCLUSIONS

Using high-purity materials and well controlled furnaces for the heat treatments, alloys equilibrated in the  $(\alpha + \gamma)$  two-phase region of the Fe-Mo and Fe-W systems have at the vertices of the  $\gamma$  loops yielded concentrations approximately 0.3 at. pct higher than obtained in previous studies. It is suggested that the new data are more reliable. They were analyzed theoretically in terms of a regular solution model and the whole phase boundaries were then calculated. The computed widths of the  $(\alpha + \gamma)$  two-phase fields agree well with those experimentally determined.

The solubility of the intermediate phases  $\mu$  and  $R$  in ferrite was studied in the binary Fe-Mo and Fe-W and the ternary Fe-Mo-W systems. The results agree fairly well with previous rough values obtained by X-ray methods or based upon microscopical observations. The new information and other relevant data were analyzed theoretically in terms of a regular solution model. The interaction energies between molybdenum and tungsten in the intermediate phases were found to be very low. An evaluation of the free energy of formation of the intermediate phases was also performed and gave the following results:

$${}^0G_{\text{Fe}_{1.5}\text{Mo}}^{\mu} - 1.5{}^0G_{\text{Fe}}^{\text{bcc}} - {}^0G_{\text{Mo}}^{\text{bcc}} = -4900 + 1.12T \quad [\text{cal mole}^{-1}]$$

$${}^0G_{\text{Fe}_{1.5}\text{W}}^{\mu} - 1.5{}^0G_{\text{Fe}}^{\text{bcc}} - {}^0G_{\text{W}}^{\text{bcc}} = 5636 - 31.25T + 3.678T \ln T \quad [\text{cal mole}^{-1}]$$

$${}^0G_{\text{Fe}_{1.7}\text{Mo}}^R - 1.7{}^0G_{\text{Fe}}^{\text{bcc}} - {}^0G_{\text{Mo}}^{\text{bcc}} = -265 - 1.99T \quad [\text{cal mole}^{-1}]$$

$${}^0G_{\text{Fe}_{1.7}\text{W}}^R - 1.7{}^0G_{\text{Fe}}^{\text{bcc}} - {}^0G_{\text{W}}^{\text{bcc}} = -867 \quad [\text{cal mole}^{-1}]$$

at 1578 K

The solubility curves for the intermediate phases in ferrite were then calculated.

The present study is an example of the method of first analyzing experimental data on phase equilibria in terms of thermodynamic models and then synthesizing the phase boundaries. It is evident, that this technique which was recently discussed by Hillert<sup>19</sup> and Kirchner *et al.*<sup>22</sup> is much more satisfactory than curve-fitting by hand but also more laborious. The present study has shown that it can be applied comfortably if machine calculations are employed.

### ACKNOWLEDGMENTS

The authors must express their appreciation to Prof. M. Hillert for his interest and comments in regard to this study. The authors are indebted to Ö. Hammar for performing many of the measurements and to T. Malmberg for preparation of the alloys. This work was supported financially by the Swedish Board for Technical Development.

### REFERENCES

1. M. Hillert, T. Wada, and H. Wada: *J. Iron Steel Inst.*, 1967, vol. 205, pp. 539-46.
2. A. K. Sinha, R. A. Buckley, and W. Hume-Rothery: *J. Iron Steel Inst.*, 1967, vol. 205, pp. 191-95.
3. A. K. Sinha and W. Hume-Rothery: *J. Iron Steel Inst.*, 1967, vol. 205, pp. 1145-49.
4. W. A. Fischer, K. Lorenz, H. Fabritius, and D. Schlegel: *Arch. Eisenhüttenw.*, 1970, vol. 41, pp. 489-98.
5. R. D. Rawlings and C. W. A. Newey: *J. Iron Steel Inst.*, 1968, vol. 206, p. 723.
6. G. Kirchner and Ö. Hammar: *Distribution of Molybdenum and Tungsten Respectively Between Ferrite and Austenite* (in Swedish). Report to the Swedish Board for Technical Development, Stockholm, 1970.
7. G. Kirchner, H. Harvig, K.-R. Moquist, and M. Hillert: *Arch. Eisenhüttenw.*, in press.
8. H. Harvig, G. Kirchner, and M. Hillert: *Met. Trans.*, 1972, vol. 3, pp. 329-32.
9. G. Kirchner, T. Nishizawa, and B. Uhrenius: *Met. Trans.*, 1973, vol. 4, pp. 167-74.
10. R. L. Orr and J. Chipman: *AIME Trans.*, 1967, vol. 239, pp. 630-33.
11. L. Kaufman: in *Phase Stability in Metals and Alloys*, P. S. Rudman, J. Stringer, and R. I. Jaffee, eds., pp. 125-50, McGraw-Hill Book Company, New York, 1967.
12. T. Nishizawa: *Thermodynamic Study of Fe-C-Mn, Fe-C-Cr and Fe-C-Mo Systems*. Report to the Swedish Board for Technical Development, Stockholm, 1966.
13. R. Schneider and R. Vogel: *Arch. Eisenhüttenw.*, 1955, vol. 26, pp. 483-90.
14. W. P. Sykes: in *Metals Handbook 1948 ed.*, T. Lyman, ed., p. 1220, The American Society for Metals, Cleveland, Ohio, 1948.
15. L. Kaufman: *Prog. Mater. Sci.*, 1969, vol. 14, pp. 55-96.
16. A. Ferrier and M. Olette: *Compt. Rend.*, 1962, vol. 254, pp. 2322-24.
17. A. W. Porter: *Trans. Faraday Soc.*, 1920-21, vol. 16, pp. 336-45.
18. T. O. Ziebold and R. E. Ogilvie: *Anal. Chem.*, 1964, vol. 36, pp. 322-27.
19. M. Hillert: in *Phase Transformations*, pp. 181-218, American Society for Metals, Metals Park, Ohio, 1970.
20. W. S. Gibson, J. R. Lee, and W. Hume-Rothery: *J. Iron Steel Inst.*, 1961, vol. 198, pp. 64-66.
21. V. Ja. Chekhovskoi, V. D. Tarasov, and I. A. Zhukova: *Teplofiz. Vys. Temp.*, Moscow, 1970, vol. 8, p. 449.
22. G. Kirchner, G. Larbo, and B. Uhrenius: in *Fortschritte in der Metallographie, Berichte der III. Internationalen Metallographie-Tagung in Leoben*, 14. bis 16. Oktober 1970, R. Mitsche, F. Jeglitsch, and G. Petzow, eds., pp. 545-57, Dr. Reiderer-Verlag, Stuttgart, 1972. *Pract. Metallogr.*, 1971, vol. 8, pp. 641-54.